applied sciences

MDPI

Article

Experimental Study of Gypsum-Concrete Dense-Column Composite Boards with External Thermal Insulation Systems

Shaochun Ma [1,2,*], Peng Bao [1,*] and Nan Jiang [3]

[1] School of Civil Engineering and Architecture, Henan University, Kaifeng 475004, China
[2] College of Water Conservancy & Environmental Engineering, Zhengzhou University, Zhengzhou 450001, China
[3] School of Civil Engineering, Tianjin University, Tianjin 300072, China; jiangnan@tju.edu.cn
* Correspondence: scma@vip.henu.edu.cn (S.M.); cnbaop@aliyun.com (P.B.)

Received: 13 February 2020; Accepted: 9 March 2020; Published: 13 March 2020

Abstract: In this paper, a new kind of gypsum-concrete dense-column thermal insulation composite board was developed, with seismic tests conducted on three specimens under quasi-static loading conditions. The fracture feature, hysteresis behavior, material strain, load-bearing and deforming capacity, and energy-dissipating capacity of the composite board were analyzed. The results indicated that this composite board has a favorable energy-dissipating capacity, i.e., relatively high seismic performance. By comparing with the experimental results of composite boards without thermal insulation systems, the influence regularity of thermal insulation system on the deformation behavior of composite board was investigated. The comparison result indicated that with a thermal insulation system, the bearing capacity and ductility of composite board are obviously increased, implying that the thermal insulation system is beneficial for the seismic performance of composite boards.

Keywords: gypsum; seismic test; dense column; external thermal insulation; hysteresis loop

1. Introduction

With the development of modern society, the energy conservation, green and environmental protection issues of buildings have gradually attracted attention [1]. Gypsum is a kind of green and non-pollutive material, with the advantages of low density, energy conservation, thermal insulation, sound isolation, fire resistance and ease of processing [2]. By adding various fibers and additives into gypsum, green building boards can be produced. Glass fiber gypsum instant large hollow boards were first developed in Australia [3]. Hollow gypsum boards are first and foremost produced in a factory and then transported to a construction site for assembly. By filling packing materials or pouring concrete into the cavities, instant composite boards are made. This kind of board can be used for both non-load-bearing and load-bearing components. As widely recognized, Australia is a country without earthquakes. Thus, the influence of earthquake has not been considered during the design and utilization of instant gypsum boards [4]. Hence, the promotion and application of gypsum composite boards become difficult in earthquake zone countries.

Countries including China and India have imported complete sets of instant gypsum board production lines from Australia. Although gypsum composite boards have many advantages, they can not be directly applied in countries in earthquake regions. To overcome this problem, many scholars have conducted massive experimental studies on the seismic performance of gypsum composite boards [5–8] and carried out related structural analyses and theoretical derivations on their structural compositions and calculation methods [9,10]. A lot of available studies have been carried out on single gypsum composite boards, which have relatively poor bearing and deformation capacity. Moreover,

the influence of thermal insulation systems has not been considered. In recent years, countries in North America and Europe have conducted a lot of investigations on gypsum-related boards and provided references for the evaluation of performances including load bearing, fire resistance, and heat storage [11–15]. However, most of these studies have considered gypsum composite boards to be non-structural components [16]. Investigations have also implied that the wall enclosure structures were key components of building energy consumption [17,18]. Hence, the most effective way to control the building energy consumption is to achieve the favorable thermal insulation performances of walls.

According to the above analyses, a gypsum-concrete dense-column composite board with thermal insulation system was proposed in this study. Composite boards with only vertical gypsum cavities and external thermal insulation systems were firstly produced in factory. The external thermal insulation system mainly consisted of thermal insulation layers and external bonding veneer gypsum protective layers. The thermal insulation layers were usually polystyrene boards, asbestos boards, and other thermal insulation boards. The composite boards were sliced into wall components according to design requirements in the factory and then transported to construction sites for assembly. Rebars were placed inside vertical gypsum cavities, which were then filled up with concrete. Thus, composite walls with load bearing capacity, thermal insulation, and enclosure function were produced. These walls improved the construction quality of external thermal insulation walls and avoided the second construction of external plaster or tile fixing of conventional wall thermal insulation layers. Thus, the shortcomings of traditional building materials, including high self-weight, great energy consumption, and single function were overcome. Moreover, outdated building crafts with shortcomings of wet hand work and labor duplication were changed. While improving the quality of houses, the dirty, difficult, risky and heavy intensities of first-line construction workers were greatly reduced.

Seismic tests were conducted on gypsum-concrete dense-column composite boards with external thermal insulation systems, with their seismic performances evaluated. By comparing to similar gypsum boards, the influence of thermal insulation system on the seismic performance of composite boards was characterized, with the performance evaluation indexes finally given. The research results can provide technical supports for the application and promotion of this composite board in earthquake region countries.

2. Experimental Overview

2.1. Specimen Design

To investigate the mechanical performances of gypsum-concrete dense-column composite boards, including bearing capacity, deformation capacity, fracture behavior, stiffness degeneration, and hysteresis performance, three specimens were designed and labeled as AA-1, AA-2 and AA-3. The specimens were 1520 mm in width and 253 mm in thickness, as shown in Figure 1. The total height of specimen was 2020 mm, including the middle composite board, bottom fixed beam, and top loading beam, as shown in Figure 2. The loading beam was embedded inside the gypsum board cavities of the composite board top, with a dimension of 220 mm × 94 mm. The gypsum ribs around the loading beam were removed to form cut-through gypsum cavities in the horizontal direction, which could be used as the non-dismantling formwork for pouring the loading beam. A fixed beam (500 mm × 403 mm) was arranged under the specimen for fixation. The two ends of the fixed beam were 250 mm longer than the specimen, which was designed to place beams while fixing the specimen. The external thermal insulation system mainly contained blue polystyrene boards with 120 mm in thickness and external bonding gypsum boards with 13 mm in thickness. The thickness of the gypsum-concrete dense-column composite board was 120 mm and could be used as the core load-bearing component of the specimen.

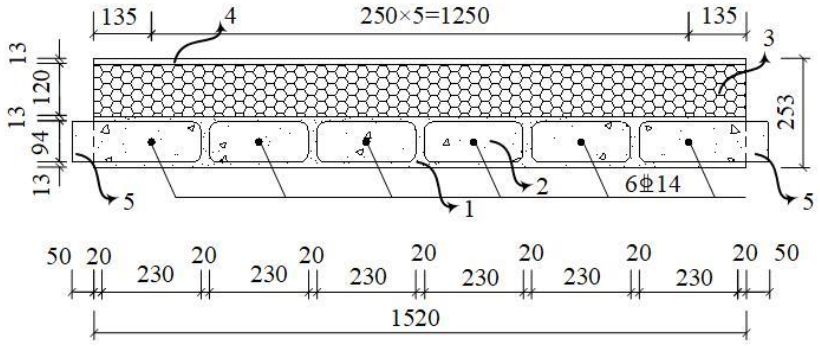

Figure 1. Plan view. Notes: 1. gypsum cavities; 2. concrete dense-column; 3. polystyrene insulation board; 4. gypsum protection board; 5. Loading position.

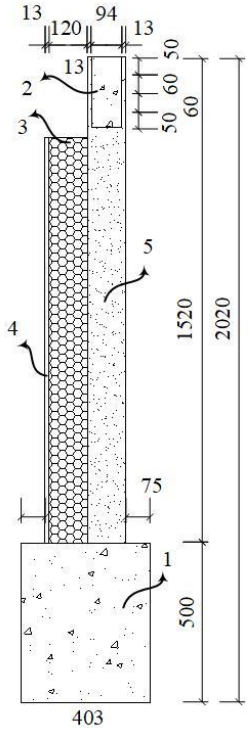

Figure 2. Elevation view. Notes: 1. fixed beam; 2. loading beam; 3. polystyrene insulation board; 4. gypsum protection board; 5. gypsum-concrete dense-column composite board.

2.2. Rebar Location

Figure 3 shows the specimen rebar location, which implies that 1C14 vertical rebars were arranged in each concrete dense column. 1C14 represents a HRB400 rebar with a diameter of 14 mm. The longitudinal rebars in the loading beam were 4C12, with stirrups of B6@200. 4C12 indicates two HRB400 rebars with a diameter of 14 mm; B6@200 represents HRB335 stirrups with a diameter of 6 mm, and the spacing is 200 mm. The rebar arrangement in the fixed beam was 4C12 longitudinal rebars with stirrups of C8@200. C8@200 represents HRB400 stirrups with a diameter of 8 mm, and the spacing is 200 mm. Vertical rebars inside the specimen were embedded into the top of the loading beam and the bottom of the fixed beam, then connected via alternate spot welding at the cross positions of rebars in the top of the loading beam. The rebar ends should also meet the requirement of anchoring.

2.3. Material Properties

During the preparation of specimens, some materials of the same batch were reserved. The mechanical parameters of each material were acquired via material tests. The compression

strength values of concrete, gypsum, and polyphenyl thermal insulation boards were measured to be 30.88, 5.52 and 0.206 MPa; and their elastic moduli were 3.27×10^4, 4350 and 2.3 MPa, respectively. The tensile strength values of rebars were 492.50 MPa (B6), 671.35 MPa (C8), 674.36 MPa (C12), 678.44 MPa (C14), and 748.07 MPa (C20), respectively.

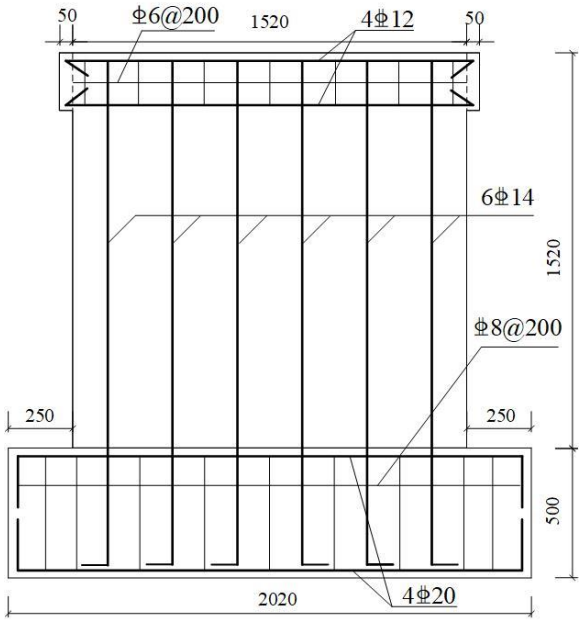

Figure 3. Specimen rebar location.

2.4. Strain Gauge Arrangement

According to previous studies, weak points usually occur in the middle and bottom of the specimen [19]. Hence, strain gauges were only placed in this area. Strain gauges were labeled as follows. A1-A5 were rebar strain gauges. B1-B4 were concrete strain gauges. C1-C9 were gypsum strain gauges in core load bearing components. D1-D3 were gypsum strain gauges in the outer area of the external thermal insulation system. By measuring material strain, the state and deformation states of each material can be determined. The arrangement of strain gauges is shown in Figure 4.

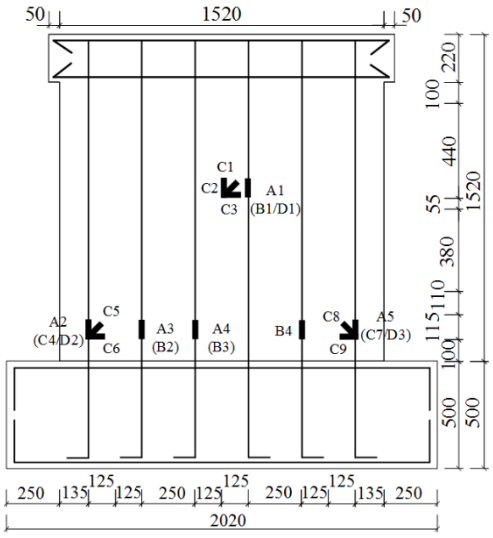

Figure 4. Strain gauge arrangement.

2.5. Experimental Method

To determine the seismic performances of the gypsum-concrete dense-column composite boards, quasi-static seismic tests were conducted on each specimen. In the loading system, the vertical and horizontal loading modes were adopted to simulate the earthquake action in the vertical and horizontal direction, as shown in Figure 5. The vertical load was decided by referring to that of a four-story residential building in engineering practice. The vertical load was calculated to be 115 kN, and the axial pressure ratio was 0.093. The vertical load was completely applied by using two 500 kN oil jacks, before the application of horizontal load. The horizontal loading was realized by using a 1000 kN push-pull jack. According to the seismic test regulation, the load-displacement mix control loading method was adopted [20]. During loading, experimental data was collected in real-time by using load sensors, displacement sensors, strain gauges, and dial-gages. By analyzing and researching the experimental results, various indexes and laws can be obtained, so as to achieve the purpose of familiarizing with the mechanical properties of gypsum-concrete dense column composite boards.

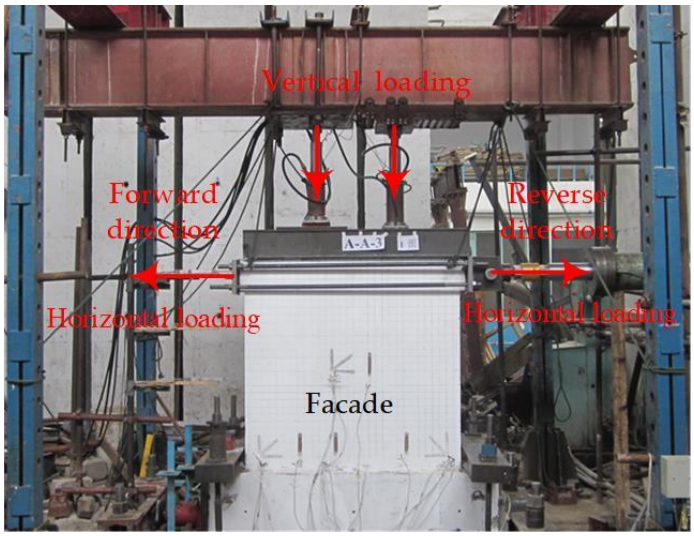

Figure 5. Experimental loading device.

3. Experimental Phenomena

By taking the 1# specimen as an example, the test procedure was described. The loading procedure control was divided into two stages: the load control stage and the displacement control stage.

3.1. Load Control Stage

Before the formal test, a preloading test was conducted in the first cycle. The formal test is to first ensure that all experimental equipment can work normally, and then start the experiment formally. The load was controlled to 30.35 and 31.40 kN in the forward and reverse direction, to ensure the smooth conduction of test. In the second cycle, the load was controlled to 50.15 and 53.40 kN in the forward and reverse direction, while no experimental phenomenon was detected. In the third cycle, the forward and reverse load values were set as 100.59 and 102.55 kN, during which, three 135° diagonal cracks occurred in the lower middle part of the specimen front (the side without thermal insulation system), and the C7 gypsum strain gauge failed. In its back facade (the outer gypsum protection board of the thermal insulation system), no crack was visible. In the fourth cycle, when the forward and reverse load values were set as 132.84 and 131.14 kN, a vertical compressed crack with a length of 63.00 cm was generated at the interface between the first concrete column and gypsum board on the right side of the facade.at the same time, a 135° crack with a length of 24 cm was generated on the left side of the back facade. In the fifth cycle, when the forward load was set as 152.84 kN,

vertical rebars in the first column yielded. Two vertical cracks occurred in the middle of the facade, with lengths of 17 and 33 cm, respectively. At the same time, the C3 gypsum strain gauge failed. When the reverse load was set to 153.40 kN, cracks in the facade-middle core column extended further, and a part of back facade polystyrene board was fractured.

3.2. Displacement Control Stage

At the top of the component, a horizontal displacement is obtained by a displacement sensor. Then, based on this value, the loading device is controlled. In the sixth cycle, the control mode was changed into displacement control. When the forward displacement was controlled to 2.47 mm, a vertical crack extending from the bottom to the middle occurred in the junction of the second core column interface in the facade. The main diagonal crack in the back facade extended to 87 cm, with a width of 3 mm. When the reverse displacement was controlled as 2.47 mm. a vertical crack extending from the bottom to the middle occurred in the junction of the third core column. In the seventh cycle, when the forward and reverse displacement values were controlled as 5.21 mm and 5.27 mm, vertical cracks with different lengths were generated in the junctions of concrete core columns, with 45°diagonal cracks extending to 85 cm. the main diagonal cracks in the back facade extended to 95 cm with a width of 6 mm. In the eighth cycle, when the forward and reverse displacement values were controlled to 7.67 mm and 7.80 mm, the tensile fracture of polystyrene boards continued to grow, and the width of the main diagonal crack reached 14.00 mm. In the ninth cycle, when the forward displacement was controlled to 9.39 mm, the core column separated from the polystyrene boards, and the horizontal load seriously decreased. When the horizontal load decreased to 85% of the ultimate load, the test was ended.

4. Results

4.1. Fracture Features

According to experiment results, specimens mainly fractured in the following modes. Vertical rebars in concrete core columns yielded. Gypsum boards between columns were compressed to fracture. Concrete in the specimen bottom was stretched or compressed to fracture. Cut-through main diagonal cracks were generated in the 45° direction. The generation and growth of cracks are analyzed below.

According to the occurrence sequence of crack in gypsum boards, the facade gypsum board started to crack in the third loading stage, while the backface gypsum board began to crack in the fourth loading stage. Hence, it is indicated that a hysteresis phenomenon existed in the crack behavior of the back facade, comparing to that of the facade. During loading, the load applying on the external thermal insulation system of the non-structural component was relatively small, while most of the load was born by the core load-bearing component of the composite board.

According to the crack development morphology of gypsum board, the facade and backface differed a lot. For example, in the seventh cycle, multiple vertical compressive cracks occurred between concrete core columns, indicating the shear stress transfer between core columns. In the backface, some orthogonally distributed 45° diagonal cracks existed, and the intervals between cracks were large. When the applied load increased to the fracture load, the morphologies of cracks in the facade and backface differed more obviously. Vertical compressive cracks in the facade cut through the gypsum board. 45° or 135° shear cracks prolonged and intersected, resulting in the partial fall-off of gypsum board. Wide main diagonal cracks extending along the 45° direction occurred in the backface and the polystyrene board was stretched to fail. When the specimen finally failed, vertical compressive cracks and shear cracks distributed in the facade, while 45° main diagonal cracks took place in the backface, with the core load-bearing components stretched to fracture along with the thermal insulation system. The fracture morphology of specimen is shown in Figure 6.

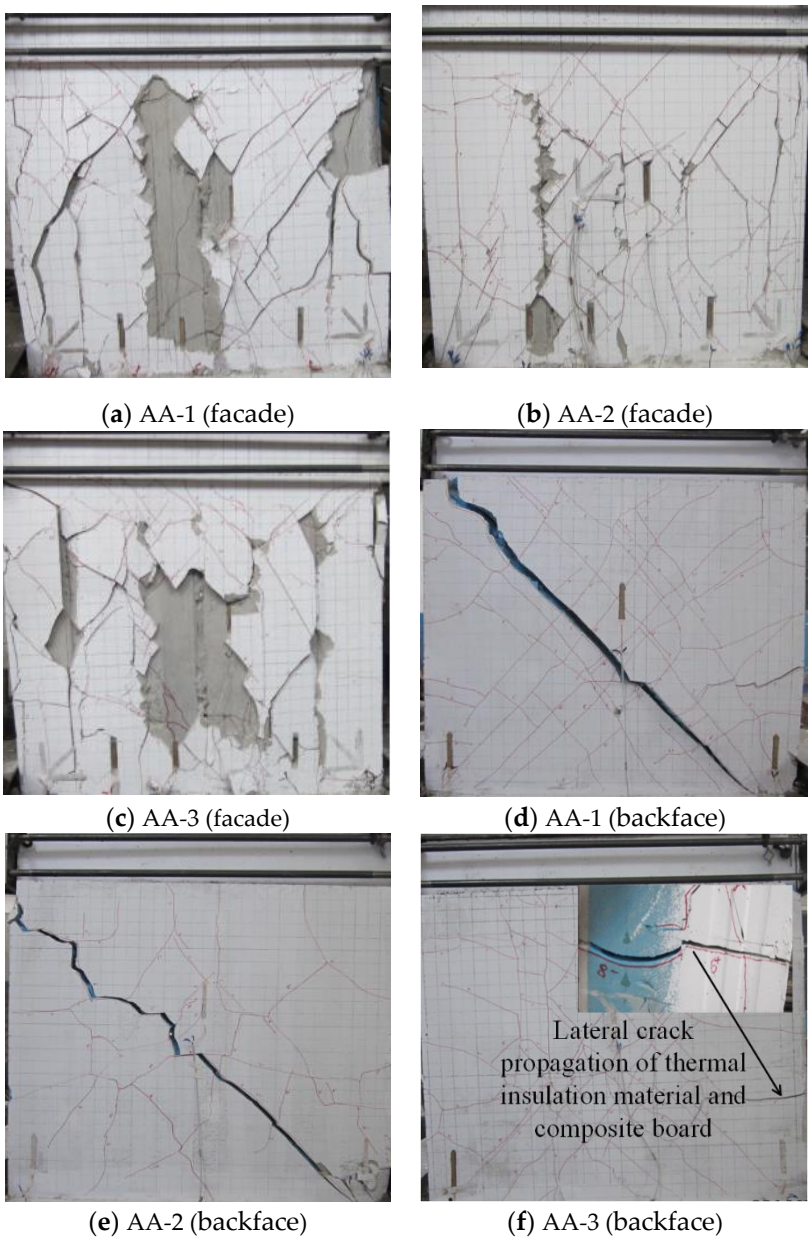

(**a**) AA-1 (facade) (**b**) AA-2 (facade)

(**c**) AA-3 (facade) (**d**) AA-1 (backface)

(**e**) AA-2 (backface) (**f**) AA-3 (backface)

Figure 6. Specimen fracture morphology.

The above analyses implied that the horizontal load didn't directly apply on the thermal insulation system of non-load bearing components. The number, length and width of cracks in the backface were obviously smaller than those in the facade. During testing, the backface gypsum board and thermal insulation board could bear some load and resist the seismic effect together with the composite board.

4.2. Hysteresis and Skeleton Curves

According to the curves in Figure 7, the specimen stiffness degraded with the increase of top displacement. Before fracturing, the specimen was in the elastic working stage. The specimen stiffness kept as a constant and the energy consumption was limited. The hysteresis loop presented the shape of a small spindle, with relatively small active area encapsulated. With the load increasing, cracks in the top columns and gypsum board generated and developed continuously. The specimen gradually yielded and accumulated damages, with the stiffness degraded notably. According to the general loading process, the shape of the hysteresis loop gradually changed from a spindle to a reverse S-shape,

presenting a serious rheostriction effect. As implied by the comparison of skeleton curves, two-stage reduction behaviors with various degrees took place. This was attributed to that, during the loading and deformation of specimen, stress redistribution took place between different materials in this zone, caused by the partial fracture or failure of materials.

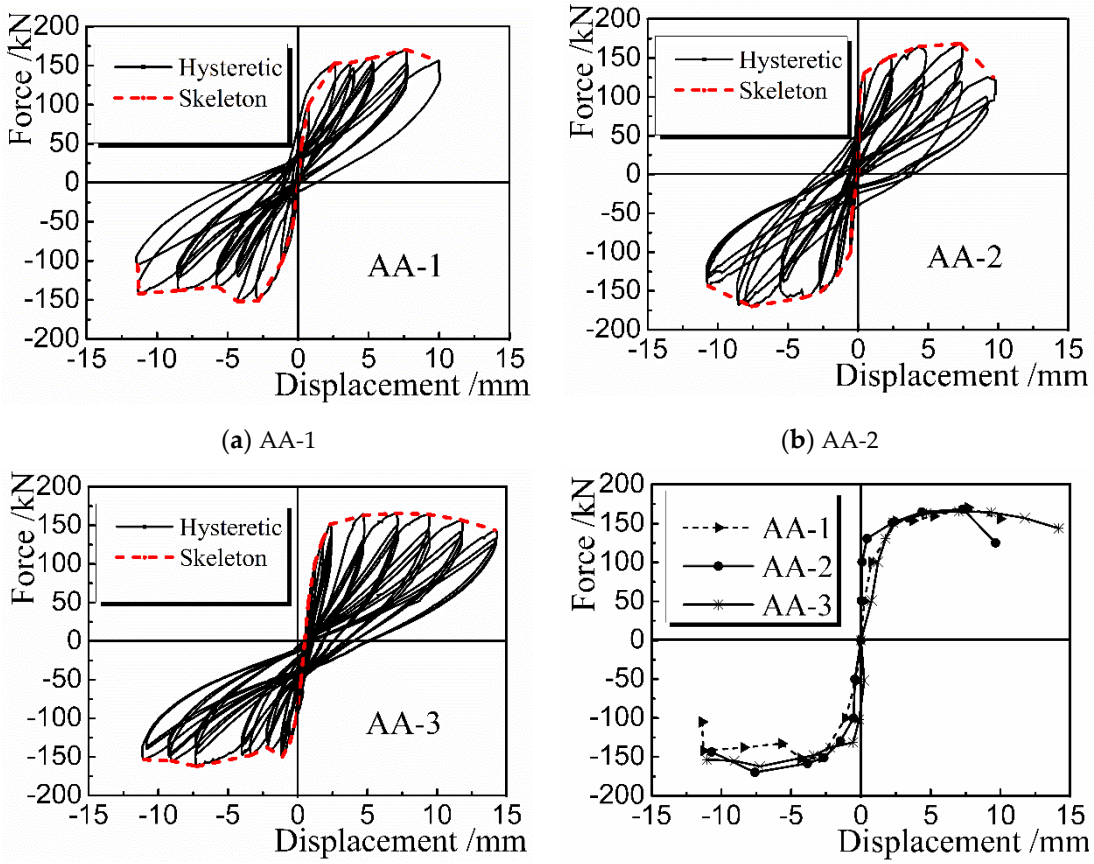

(**a**) AA-1 (**b**) AA-2

(**c**) AA-3 (**d**) Comparison of skeleton curves

Figure 7. Hysteresis and skeleton curves.

4.3. Material Strain Analysis

To investigate the strain variation regularity of the gypsum-concrete dense-column composite board with external thermal insulation system, Strain gauges with materials corresponding to typical positions in the specimen were selected as the research object, i.e., rebar strain gauge A2, concrete strain gauge B2, gypsum board strain gauge on the side without thermal insulation system C4, and external gypsum board strain gauge B2. All material strain gauges were placed at the same height. The lateral distances between B2, A2, C4, and D2 were all 250 mm. Hence, their positions could be approximated as the same. Based on the test results, the most lateral rebars and concrete yielded or fractured in the fifth loading stage. Hence, in this paper, only the load-strain curves of different materials before strain gauge failure in the first five loading stages were demonstrated, as shown in Figure 8.

In the initial loading and deformation stage, the specimen stayed in the elastic deformation region due to the limited external load. According to the load-strain curves of rebar, concrete, and gypsum in the facade and backface, the variation and development of different materials strains were synchronized with a limited difference. When the typical positions were stretched or compressed, the material strains were all between −50 and +50. With the load increased to the concrete fracture limit, the concrete cracked. Most of the load previously born by the concrete transferred to rebars and gypsum boards nearby also shared some load. The gypsum board failed after the concrete, indicating that glass fibers in the gypsum board enhanced the tensile strength in the early stage of cracking.

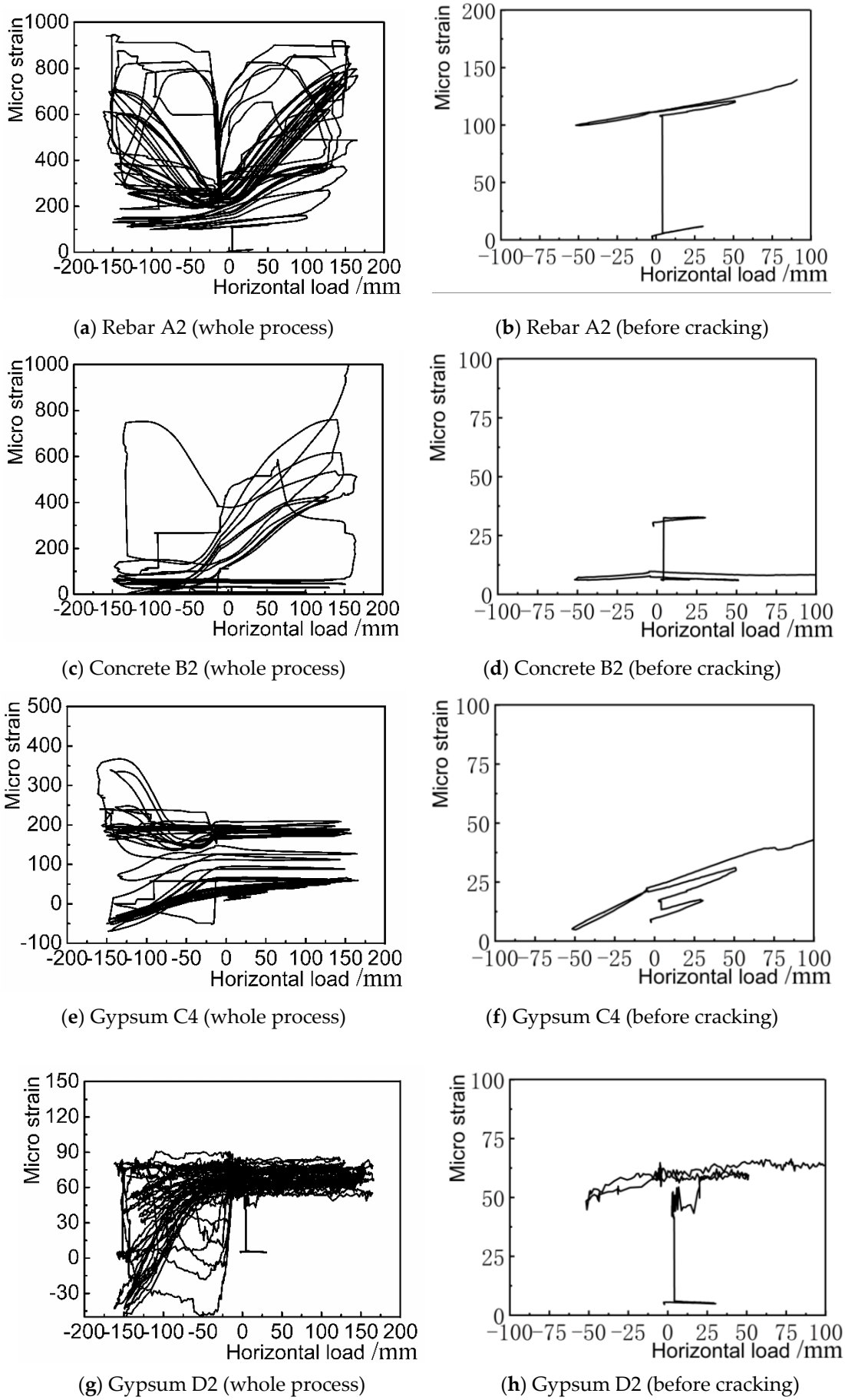

(**a**) Rebar A2 (whole process)

(**b**) Rebar A2 (before cracking)

(**c**) Concrete B2 (whole process)

(**d**) Concrete B2 (before cracking)

(**e**) Gypsum C4 (whole process)

(**f**) Gypsum C4 (before cracking)

(**g**) Gypsum D2 (whole process)

(**h**) Gypsum D2 (before cracking)

Figure 8. Load-strain curves.

According to the overall variation tendency of the load-strain curves of concrete and gypsum, the strain variation was large under tensile forces and experienced sharp increase. Meanwhile, under the compressive load, the strain varied little without an abrupt increase. Thus, it is implied that brittle materials such as concrete and gypsum entered the elastoplastic deformation easier under tensile stress, than under compressive stress. Accordingly, cracks also occurred earlier.

By comparing the load-strain curves of gypsum on two sides of the specimen, the micro strain range of gypsum board was [−60, +350] in the facade while [−50, +75] in the backface. According to the micro strain range, it can be found that the load applying on the facade gypsum board was much greater than that on the backface. Thus, under reciprocated loading, the load was mainly born by the core load-bearing components, while the load applying on the nonstructural component thermal insulation system was limited.

4.4. Load Bearing and Deformation Capacity

Test results of the load bearing and deformation capacity of key points are listed in Table 1. According to the seismic test regularity [21], the ultimate load Pu born by the specimen was the load corresponding to the condition when the specimen bore the maximum load. The ultimate displacement Δu of the specimen was the deformation under the effect of the ultimate load. The crack load P_{cr} and crack deformation Δ_{cr} were the load and crack of the initial specimen cracking; the yield load P_y and yield deformation Δy were the load and deformation during specimen yielding. The crack load, yield load, and ultimate load of the gypsum-concrete dense-column composite board were 86.31 kN, 150.52 kN and 168.32 kN. The corresponding deformation was 0.44 mm, 2.38 mm, and 7.34 mm, respectively. These values are the average of the key points on the three sample skeleton curves. The purpose is to easily evaluate the mechanical properties of similar samples. It is implied that both the load and deformation increased nonlinearly. The ultimate load bearing capacity of this composite board was 8.59% higher than that of the composite board (155 kN) described in Ref. [22], which only had vertical gypsum channels, while no thermal insulation system was adopted. Accordingly, the ductility coefficient was improved by 76%, comparing to the 1.75 in Ref. [22]. Hence, it is implied that by adding external thermal insulation system to the gypsum-concrete dense-column composite board, the entire load bearing and deformation performance of the composite board was improved. The ductility coefficient of 3.08, which is greater than those of similar boards, indicates that this board type has better seismic performances.

Table 1. Load bearing and deformation.

Specimen No.	P_{cr} (kN)	Δ*cr* (mm)	P_y (kN)	Δ*y* (mm)	P_u (kN)	Δ*u* (mm)	*u*
AA-1	82.47	0.44	152.84	2.47	170.58	7.67	3.11
AA-2	85.81	0.46	151.12	2.34	168.55	7.33	3.13
AA-3	90.66	0.43	147.61	2.34	165.84	7.02	3.00
Avg.	86.31	0.44	150.52	2.38	168.32	7.34	3.08

4.5. Energy Dissipation Capacity

According to previous studies, the composite board absorbs energy during loading and releases energy during unloading [23]. The effective area of the hysteresis loop is usually adopted as the index to evaluate the specimen energy dissipation capacity [24]. The viscous damping coefficient h_e and power ratio coefficient I_W^S are listed in Table 2. The viscous damping coefficients of 1Δy, 2Δy, and 3Δy are 0.092, 0.117, and 0.148, respectively. The viscous damping coefficient increased with the increase of displacement circulation, indicating that the plastic deformation capacity and energy-dissipating capacity of the specimen were rising. The power output ratios corresponding to 1Δy, 2Δy, and 3Δy are 1.000, 4.171 and 8.815, respectively. It is demonstrated that the power output ratio gradually increases with the increase of displacement circulation; that is, the energy absorbed by the component during

each stage of displacement circulation is greater than that in the previous stage. Thus, the energy absorption capacity of the component is improved, and the specimen has favorable seismic energy dissipation energy.

Table 2. Viscous damping coefficient and power ratio coefficient.

Specimen No.	Viscous Damping Coefficient h_e			Power Ratio Coefficient I_W^S		
	1Δy	2Δy	3Δy	1Δy	2Δy	3Δy
AA-1	0.090	0.105	0.141	1.000	4.189	8.633
AA-2	0.096	0.116	0.147	1.000	4.173	9.090
AA-3	0.090	0.129	0.156	1.000	4.151	8.722
Avg.	0.092	0.117	0.148	1.000	4.171	8.815

Notes: 1Δy, 2Δy and 3Δy denotes 1, 2 and 3 times of yield displacement, respectively.

5. Conclusions

In this paper, the low-cycle cyclic tests of three gypsum-concrete dense-column composite boards with external thermal insulation systems were conducted, with the seismic performance characterized and compared with similar boards.

1. On the basis of composite boards only having vertical gypsum cavities, the influence of external thermal insulation system was considered, and a new kind of gypsum-concrete dense-column thermal-insulation composite board was developed. Under the influence of tensile-compressive cyclic load, the repetitive open-close feature of gypsum cracks between concrete dense columns can effectively absorb earthquake energy, which is beneficial to the improvement of seismic performance.
2. Horizontal earthquake action is directly applied on the core load-bearing component of the composite board. The deformation results in the specimen facade (length or width of crack, partial fall-off of gypsum, etc.) are more sensitive than those in the backface. The thermal insulation board and gypsum guard board can bear some load and resist the earthquake action together with the composite board.
3. Based on the load-strain analysis of composite board, it is demonstrated that when the typical zone is stretched, the material strain is relatively large, which becomes relatively small in compressed zones. Thus, it is implied that brittle materials such as concrete and gypsum enter the elastoplastic deformation easier under tensile stress than under compressive stress. In the early stage of cracking, fibers in the gypsum board present some tensile resistance.
4. By comparing to similar composite boards of the literature [22] without thermal insulation system, the load bearing capacity and ductility of the board developed in this study are increased by 8.59% and 76%, indicating that this composite board has favorable seismic performances.

Author Contributions: S.M. performed the tests, analyzed the data and wrote the paper. P.B. and N.J. conceived and supervised the work. All authors contributed to conclusion of the thesis. All authors have read and agreed to the published version of the manuscript.

Funding: The authors would like to express heartfelt gratitude to the financial support by the Science Technology of the Ministry of Housing and Urban-Rural Development (No. 2018-K9-065), China Postdoctoral Science Foundation funded project (No. 2018M632805), Foundation of He'nan Educational Committee (18A560007), and key scientific and technological project of Henan Province (No. 182102210234).

Conflicts of Interest: The authors declare no conflict of interest.

References

1. Zhang, X.H.; Wang, R.H.; Xu, M.; Zhang, E.Y. Anti-seismic experimental study on thin-walled steel composite wall with one-sided cladding of strawboard. *Buil. Mater.* **2019**, *22*, 908–916.

2. Ma, S.C.; Bao, P.; Iang, X.L.; Li, N.N. Experiment on anti-seismic performance of assembled energy-saving shear wall. *Lanzhou Univ. Technol.* **2019**, *45*, 113–117.
3. Wu, Y.F. The effect of longitudinal reinforcement on the cyclic shear behavior of glass fiber reinforced gypsum wall panels: Tests. *Eng. Struct.* **2004**, *26*, 1633–1646. [CrossRef]
4. Graziotti, F.; Tomassetti, U.; Penna, A.; Magenes, G. Out-of-plane shaking table tests on URM single leaf and cavity walls. *Eng. Struct.* **2016**, *125*, 455–470. [CrossRef]
5. Ma, S.C.; Bao, P.; Iang, X.L.; Li, N.N. Seismic Test Research of Prefabricated Building Wallboard. *Henan Univ. (Nat. Sci.)* **2018**, *48*, 717–722.
6. Ma, S.C.; Jang, N. Experimental investigation on the seismic behavior of a new-type composite interior wallboard. *Mater. Struct.* **2016**, *49*, 5085–5095. [CrossRef]
7. Selvaraj, S.; Madhavan, M. Improvements in AISI Design Methods for Gypsum-Sheathed Cold-Formed Steel Wall Panels Subjected to Bending. *Struct. Eng.* **2019**, *145*, 04018243. [CrossRef]
8. Fiorino, L.; Shakeel, S.; Macillo, V.; Landolfo, R. Seismic response of CFS shear walls sheathed with nailed gypsum panels: Numerical modelling. *Thin-Walled Struct.* **2018**, *122*, 359–370. [CrossRef]
9. Jiang, N.; Ma, S.C. Simplified Calculation Model and Experimental Study of Latticed Concrete-Gypsum Composite Panels. *Materials* **2015**, *8*, 7199–7216. [CrossRef]
10. Macillo, V.; Fiorino, L.; Landolfo, R. Seismic response of CFS shear walls sheathed with nailed gypsum panels: Experimental tests. *Thin-Walled Struct.* **2017**, *120*, 161–171. [CrossRef]
11. Ercolino, M.; Ricci, P.; Magliulo, G.; Verderame, G.M. Influence of infill panels on an irregular RC building designed according to seismic codes. *Earthq. Struct.* **2016**, *10*, 261–291. [CrossRef]
12. Lafontaine, A.; Chen, Z.; Doudak, G.; Chui, Y.H. Lateral Behavior of Light Wood-Frame Shear Walls with Gypsum Wall Board. *Struct. Eng.* **2017**, *143*, 04017069. [CrossRef]
13. Soroushian, S.; Maragakis, E.M.; Ryan, K.L.; Sato, E.; Sasaki, T.; Okazaki, T.; Mosqueda, G. Seismic Simulation of an Integrated Ceiling-Partition Wall-Piping System at E-Defense. II: Evaluation of Nonstructural Damage and Fragilities. *Struct. Eng.* **2016**, *142*, 04015131. [CrossRef]
14. Way, D.; Sinha, A.; Kamke, F.A. Performance of Light-Frame Timber Shear Walls Produced with Weathered Sheathing. *Arch. Eng.* **2020**, *26*, 04019019. [CrossRef]
15. Lafontaine, A.; Doudak, G. Stiffness model for gypsum wallboard-to-wood joints. *Can. Civ. Eng.* **2017**, *44*, 338–347. [CrossRef]
16. Rahmanishamsi, E.; Soroushian, S.; Maragakis, E.; Sarraf Shirazi, R. Analytical Model to Capture the In-Plane and Out-of-Plane Seismic Behavior of Nonstructural Partition Walls with Returns. *Struct. Eng.* **2017**, *143*, 04017033. [CrossRef]
17. Sharifi, N.P.; Shaikh, A.A.N.; Sakulich, A.R. Application of phase change materials in gypsum boards to meet building energy conservation goals. *Energy Build.* **2017**, *138*, 455–467. [CrossRef]
18. Karaipekli, A.; Sarı, A. Development and thermal performance of pumice/organic PCM/gypsum composite plasters for thermal energy storage in buildings. *Sol. Energy Mater. Sol. Cells* **2016**, *149*, 19–28. [CrossRef]
19. Ma, S.C.; Iang, N. Seismic experimental study on new-type composite exterior wallboard with integrated structural function and insulation. *Materials* **2015**, *8*, 3732–3753. [CrossRef]
20. *JGJ101-96 Specification of Testing Methods for Earthquake Resistant Building*; Chinese Building Industry Press: Beijing, China, 1997.
21. *JGJ/T101-2015 Specification of Seismic Test of Buildings*; Chinese Building Industry Press: Beijing, China, 2015.
22. Yue, W.; Iang, X.L.; Gu, Y. Test of shear performance of rapid walls. *Huazhong Univ. Sci. Technol. Urban Sci. Ed.* **2006**, *23*, 27–30.
23. Polastri, A.; Izzi, M.; Pozza, L.; Loss, C.; Smith, I. Seismic analysis of multi-storey timber buildings braced with a CLT core and perimeter shear-walls. *Bull. Earthq. Eng.* **2019**, *17*, 1009–1028. [CrossRef]
24. Scotta, R.; Marchi, L.; Trutalli, D.; Pozza, L. A Dissipative Connector for CLT Buildings: Concept, Design and Testing. *Materials* **2016**, *9*, 139. [CrossRef] [PubMed]